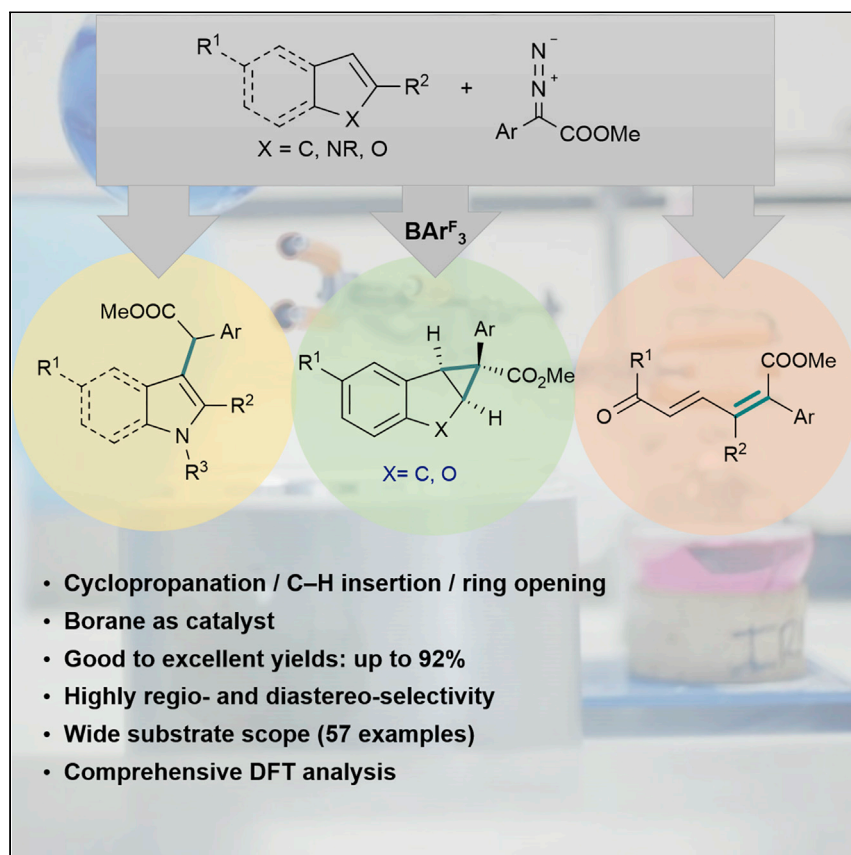


## Article

## Borane-Catalyzed Stereoselective C–H Insertion, Cyclopropanation, and Ring-Opening Reactions



This work demonstrates the highly selective metal-free catalytic reactions of  $\alpha$ -aryl  $\alpha$ -diazoesters with a range of (hetero)cycles and olefins using Lewis acidic boranes. The simple, mild reaction protocol employed represents an alternative to the commonly used precious metal systems and may provide future applications in the generation of biologically active compounds.

Ayan Dasgupta, Rasool Babaahmadi, Ben Slater, Brian F. Yates, Alireza Ariaferd, Rebecca L. Melen

melen@cardiff.ac.uk

## HIGHLIGHTS

Borane-catalyzed regio- and diastereo-selective reactions

Selective C–H insertion, cyclopropanation, or ring-opening reaction

57 examples with isolated yields up to 92%

Detailed DFT analysis to explain reaction mechanisms and selectivity



Article

# Borane-Catalyzed Stereoselective C–H Insertion, Cyclopropanation, and Ring-Opening Reactions

Ayan Dasgupta,<sup>1</sup> Rasool Babaahmadi,<sup>2</sup> Ben Slater,<sup>3</sup> Brian F. Yates,<sup>2</sup> Alireza Ariaifard,<sup>2</sup> and Rebecca L. Melen<sup>1,4,\*</sup>

## SUMMARY

Lewis acidic boranes have been shown to be effective metal-free catalysts for highly selective reactions of donor-acceptor diazo compounds to a range of substrates. The reactions of  $\alpha$ -aryl  $\alpha$ -diazoesters with nitrogen heterocycles indole or pyrrole selectively generate C3 and C2 C–H insertion products, respectively, in good to excellent yields even when using unprotected indoles. Alternatively, benzofuran, indene, and alkene substrates give exclusively cyclopropanated products with  $\alpha$ -aryl  $\alpha$ -diazoesters, whereas the reactions with furans lead to ring-opening. Comprehensive theoretical calculations have been used to explain the differing reactivities and high selectivities of these reactions. Overall, this work demonstrates the selective metal-free catalytic reactions of  $\alpha$ -aryl  $\alpha$ -diazoesters with (hetero)cycles and alkenes. This simple, mild reaction protocol represents an alternative to the commonly used precious metal systems and may provide future applications in the generation of biologically active compounds.

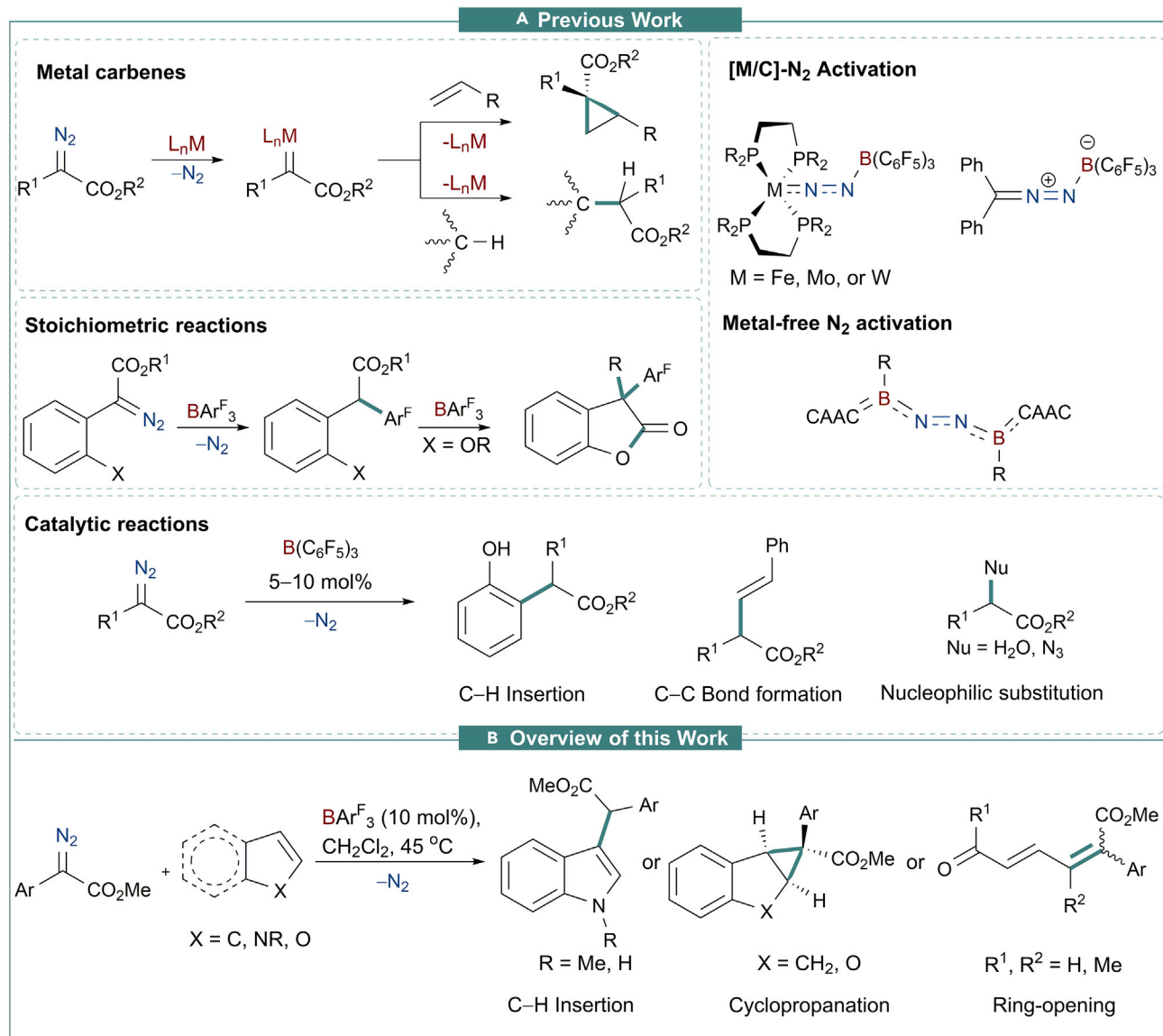
## INTRODUCTION

The presence and availability of *d*-orbitals on transition metals has rendered them indispensable for a vast number of transformations in which synergic bonding and back-bonding interactions are central to their chemistry. It is these bonding properties that allow metal-carbene complexes to play an important role in organometallic and synthetic chemistry.<sup>1</sup> In particular, one area that remains at the forefront of both academic and industrial research is the use of metal carbene complexes as intermediates in the functionalization of electron-rich oxygen and nitrogen heterocycles that are omnipresent in nature.<sup>2</sup> One popular method to generate such complexes is the catalytic decomposition of diazo compounds.<sup>3</sup> The metal-carbene complex can subsequently be used in a plethora of carbene transfer reactions including C–H insertion<sup>4</sup> and cyclopropanation<sup>5</sup> (Scheme 1A). (Di)rhodium complexes<sup>6</sup> are typically the metal catalyst of choice although other precious metal catalysts such as gold,<sup>7</sup> ruthenium,<sup>8</sup> palladium,<sup>9</sup> and iridium<sup>10</sup> can be employed. Of the first-row transition metals, copper<sup>11</sup> is also commonly used, and recently, the earth-abundant metal, iron,<sup>12</sup> has also been shown to be an effective catalyst for carbene transfer reactions. Recently, it has been shown that the photocatalyzed activation of diazo-compounds is also possible for cyclopropanation or C–H activation of olefins and heteroarenes.<sup>13</sup>

Although rhodium is typically used, one major pitfall includes its high cost and inherent toxicity.<sup>14</sup> One field of research that has flourished over the last decade is

## The Bigger Picture

Efficient and facile routes to heterocyclic compounds are highly desirable because of their remarkable biological importance and applications in drugs approved by the Food and Drug Administration. Current synthetic routes frequently use precious metal-catalyzed reactions. The problems associated with the limited resources of precious metals as well as their toxicities can be avoided through metal-free approaches. Our investigations on the reactivities of diazoesters toward the (hetero)arenes reveal that by using Lewis acidic triarylboranes as a catalyst, we can selectively effect C–H insertion, cyclopropanation, or ring-opening in good to excellent yields. Main group, or metal-free, catalysis has become a burgeoning field; yet, this flourishing field is still in its nascent stage. The work described herein represents a step toward improving the applicability of main group catalysis by employing metal-free approaches in the functionalization of organic compounds.



**Scheme 1. Previous and Current Work**

(A) Previous work on metal-carbene transfer reactions and borane activation of dinitrogen compounds.

(B) Work described herein. CAAC, cyclic (alkyl)(amino)carbene; Ar<sup>F</sup>, C<sub>6</sub>F<sub>5</sub>, 2,4,6-F<sub>3</sub>C<sub>6</sub>H<sub>2</sub>, or 3,4,5-F<sub>3</sub>C<sub>6</sub>H<sub>2</sub>.

main group chemistry in which current studies aim to unearth new reactivities and selectivities using metal-free compounds, thereby providing alternative (or complementary) catalysts to those based on the d-block elements.<sup>15</sup> One area that has received attention is the applications of Lewis-acidic-fluorinated triarylboranes in small-molecule activation and catalysis following the seminal work of Piers in 1996 who showed that B(C<sub>6</sub>F<sub>5</sub>)<sub>3</sub> could be used as an effective catalyst for hydrosilylation reactions.<sup>16</sup> Later, this borane and its derivatives were also employed as the Lewis acid component of frustrated Lewis pairs (FLPs) to effect metal-free hydrogenation.<sup>17</sup> More recently, the use of boranes for the activation of N–N bonded compounds has garnered momentum,<sup>18</sup> particularly since the groundbreaking work by Braunschweig on the first-ever metal-free activation of dinitrogen in 2018.<sup>19</sup> Specifically, BAr<sup>F</sup><sub>3</sub> (Ar<sup>F</sup> = C<sub>6</sub>F<sub>5</sub>, 2,4,6-F<sub>3</sub>C<sub>6</sub>H<sub>2</sub>, 3,4,5-F<sub>3</sub>C<sub>6</sub>H<sub>2</sub>) have been reported to activate metal

<sup>1</sup>Cardiff Catalysis Institute, School of Chemistry, Cardiff University, Main Building, Park Place, Cardiff CF10 3AT, UK

<sup>2</sup>School of Natural Sciences-Chemistry, University of Tasmania, Private Bag 75, Hobart, Tasmania 7001, Australia

<sup>3</sup>Department of Chemistry, University College London, London WC1H 0AJ, UK

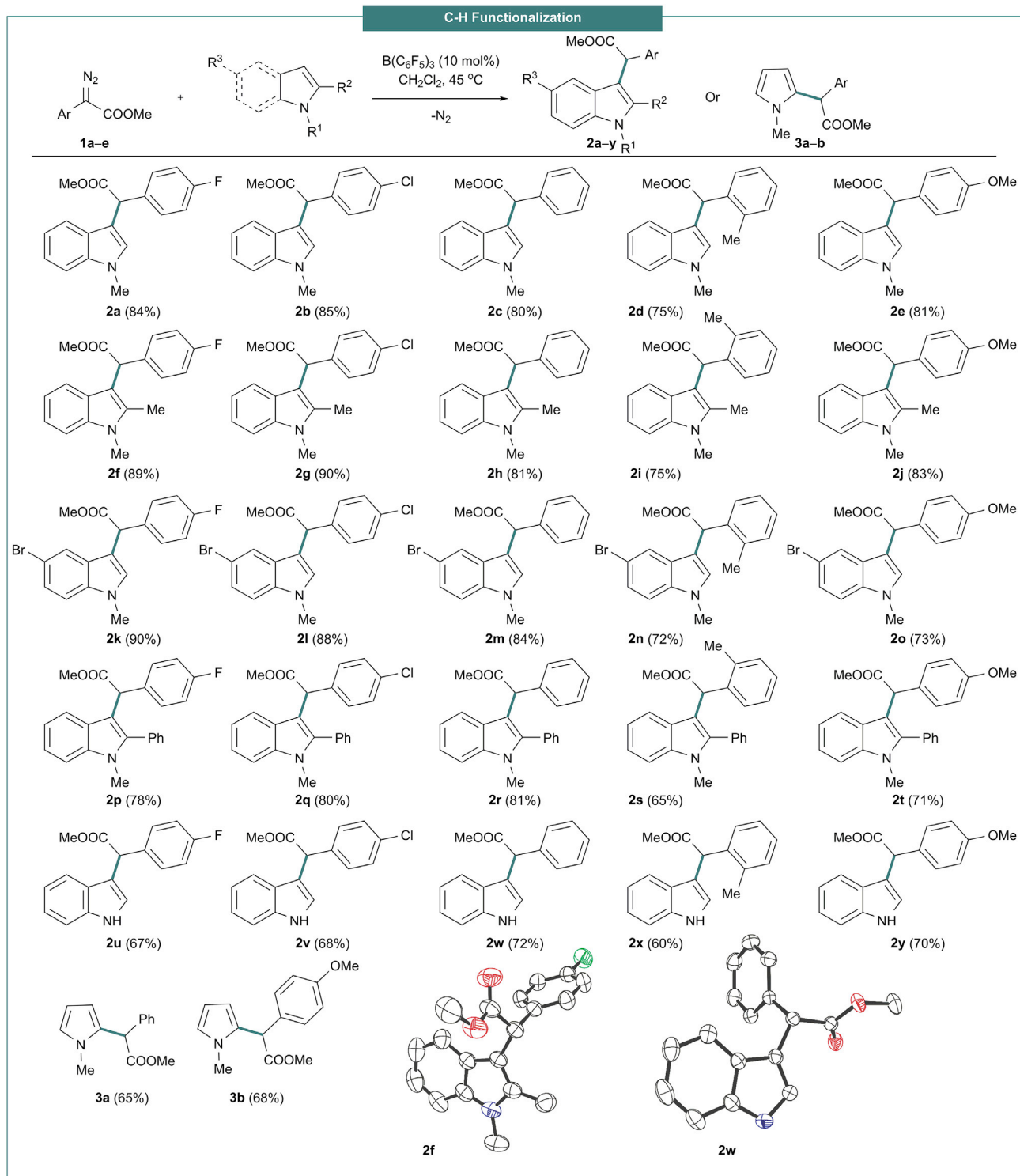
<sup>4</sup>Lead Contact

\*Correspondence: [melenr@cardiff.ac.uk](mailto:melenr@cardiff.ac.uk)  
<https://doi.org/10.1016/j.chempr.2020.06.035>

dinitrogen compounds<sup>20</sup> and diazo compounds.<sup>21,22</sup> The latter, however, are typically stoichiometric, whereby the carbene generated inserts into a B–C bond, leading to  $\alpha$ -functionalized carbonyl compounds.<sup>21,23</sup> We have recently employed this reactivity in the metal-free synthesis of asymmetric 3,3-disubstituted benzofuran-2(3H)-ones from the reaction between  $\alpha$ -aryl  $\alpha$ -diazoacetates and triarylboranes.<sup>21</sup> Recently, there have been a few reports that show that  $B(C_6F_5)_3$  can activate diazo-compounds in a catalytic manner. Specifically,  $\alpha$ -aryl  $\alpha$ -diazoesters have been demonstrated to be suitable substrates for insertion and nucleophilic substitution reactions (Scheme 1A). In 2016, Zhang reported the *ortho*-selective C–H alkylation of unprotected phenols with  $\alpha$ -aryl  $\alpha$ -diazoesters using 5 mol %  $B(C_6F_5)_3$ .<sup>24</sup> Mechanistic studies revealed that the high selectivity for the *ortho*-position was due to a hydrogen-bond directed process involving the O–H group of the phenol, thereby explaining why substrates such as anisole did not work well for these reactions. Although these boranes are moisture sensitive (due to their strong Lewis acidic character that often results in B–C bond protonolysis), water in combination with  $B(C_6F_5)_3$  was found to be a suitable catalyst for the O–H insertion reactions of water with  $\alpha$ -aryl  $\alpha$ -diazoesters.<sup>25</sup> Interestingly, mechanistic studies indicate that in this case,  $B(C_6F_5)_3 \cdot nH_2O$  acts as a Brønsted acid rather than a Lewis acid catalyst to facilitate a nucleophilic substitution mechanism. In a very similar vein, water could be replaced by azide for this type of nucleophilic substitution, but the mechanism was proposed to proceed through Lewis acid activation of the  $N_2$  functionality.<sup>26</sup> Finally, Prabhu et al. have demonstrated the use of catalytic  $B(C_6F_5)_3$  toward C–C bond functionalization of aryl-allyl alcohols using donor-acceptor carbenes, which was suggested to progress through borane activation of the diazo functionality followed by borane-carbene adduct formation.<sup>27</sup>

As can be seen above, several different modes of activation of diazo-compounds using  $B(C_6F_5)_3$  have been proposed, and a few computational studies have shed some light on the probable reaction mechanisms. Density functional theory (DFT) studies reported by Stephan<sup>28</sup> for the reaction of  $Ph_2CN_2$  with  $B(C_6F_5)_3$  revealed the mechanism for this reaction is the initial activation of the  $N_2$  functionality through Lewis adduct formation. This is followed by  $N_2$  release to generate a carbene-borane adduct (calculated to be exergonic by about 53 kcal/mol).<sup>28</sup> Subsequent, computational studies by Wu<sup>29</sup> on the  $B(C_6F_5)_3$  activation of diazoesters also revealed  $N_2$  release, but in this case, activation of the carbonyl to generate a borane-diazoester conjugated adduct was more favorable than activation of the  $N_2$  functionality.<sup>29</sup> The electron-withdrawing effect of Lewis acidic  $B(C_6F_5)_3$  makes this adduct susceptible toward selective electrophilic attack.

It was our hypothesis that we could utilize Lewis acidic boranes as an effective catalyst in the activation of diazo compounds for a range of reactions as an alternative to metal-catalyzed processes. Herein, we report the high regio- and diastereo-selective C–H insertion, cyclopropanation, and ring-opening reactions of a range of substrates including indoles, benzofurans, indenes, pyrroles, styrenes, and furans under mild conditions (Scheme 1B). In particular, we showcase that these reactions work well on unprotected indoles contrary to many metal-catalyzed reactions, thereby removing the requirement for additional reaction steps (protection and deprotection) in chemical synthesis. We also report the mechanisms of these reactions using comprehensive DFT studies to fully understand both our observed regio- and diastereoselectivity.



### Scheme 2. Scope of C–H Insertion of N-Heterocycles

Conditions: diazoester (1 equiv), indole/pyrrole (1.1 equiv), and  $B(C_6F_5)_3$  (10 mol %) in  $CH_2Cl_2$  (1.5 mL) at  $45^\circ C$ . Bottom right: solid-state structures of **2f** (left) and **2w** (right). Thermal ellipsoids are drawn at 50% probability. H atoms omitted for clarity. All the yields reported are isolated yields.

## RESULTS AND DISCUSSION

$\alpha$ -Aryl  $\alpha$ -diazoesters (**1a–e**, Scheme 2; Figures S1–S11) bearing electron-withdrawing and electron-donating functional groups were initially prepared using standard literature procedures.<sup>30</sup> Addition of fluorinated triarylboranes  $\text{BAr}^{\text{F}}_3$  ( $\text{Ar}^{\text{F}} = \text{C}_6\text{F}_5$ , 2,4,6- $\text{F}_3\text{C}_6\text{H}_2$ , or 3,4,5- $\text{F}_3\text{C}_6\text{H}_2$ ) to **1** led to the rapid release of  $\text{N}_2$ . As demonstrated in our previous studies, as well as those by Stephan, under stoichiometric conditions, the resulting carbene inserts into one of the B–C bonds, ultimately leading to a boron enolate.<sup>21,22c</sup> If, however, the loading of borane is reduced to 10 mol %, then dimerization of the carbene is observed by  $^1\text{H}$  NMR spectroscopy and X-ray diffraction. These promising results demonstrated that boranes can be used as a catalyst to activate diazo-compounds and indicated that they could be used as an alternative to metal carbenes as intermediates in the functionalization of various organic compounds. This prompted us to explore the reactivity of  $\alpha$ -aryl  $\alpha$ -diazoesters (**1a–e**) with various heterocycles, indenes, and styrenes catalyzed by boranes.

### C–H Insertion, Cyclopropanation, and Ring-Opening

Indoles are ubiquitous in nature, possess many biological activities, and are common motifs in many drugs and agrochemicals.<sup>31</sup> As such, methods to modify indoles are highly sought after. One method to achieve this is through a transition-metal-catalyzed carbene transfer reaction to yield C3-substituted compounds.<sup>32</sup> We therefore decided to start our investigations into the borane-catalyzed carbene transfer reactions using *N*-methylindole as the substrate in reactions with  $\alpha$ -aryl  $\alpha$ -diazoester **1a** (Scheme 1). Optimization of the reaction conditions (see Table S1) revealed that by using 10 mol % of the borane  $\text{B}(\text{C}_6\text{F}_5)_3$ , 84% yield of the C3-substituted product **2a** could be formed after 22 h in  $\text{CH}_2\text{Cl}_2$  at 45°C. Reducing the Lewis acidity by using  $\text{B}(2,4,6\text{-F}_3\text{C}_6\text{H}_2)_3$  as a catalyst afforded the desired product in 76% yield, whereas  $\text{B}(3,4,5\text{-F}_3\text{C}_6\text{H}_2)_3$  gave 56% isolated yield. Lowering the catalytic loading of  $\text{B}(\text{C}_6\text{F}_5)_3$  to 5 mol % also led to full conversion albeit with longer reaction times of 32 h. Under the optimized reaction conditions (10 mol %  $\text{B}(\text{C}_6\text{F}_5)_3$ , 45°C,  $\text{CH}_2\text{Cl}_2$ ), various indoles and  $\alpha$ -aryl  $\alpha$ -diazoesters were investigated in the C–H insertion reaction to give the C3-substituted indole as the sole product (Scheme 2). Indeed, deuterium-labeling studies using 1,2-dimethylindole-3-*D* or 1-methylindole-2-*D* with **1a** clearly revealed the reaction was proceeding through carbene insertion into the C–H/D bond at the C3 position (see Figures S67–S76; Scheme S1). The influence of the electron-donating or electron-withdrawing group attached to the aryl ring of the  $\alpha$ -aryl  $\alpha$ -diazoester (**1a–e**) was investigated but appeared to have little effect on the rate or yield of the reaction with products **2a–e** (Figures S12–S22), displaying excellent isolated yields from 75% to 85% when reacted with *N*-methylindole. Likewise, indole starting materials bearing substitution on the phenyl ring as well as at the C2 position were tested including 1,2-dimethylindole, 5-bromo-1-methylindole, and 1-methyl-2-phenylindole, which afforded the desired C–H insertion products (**2f–t**, Figures S23–S55) in excellent yields (up to 90%).

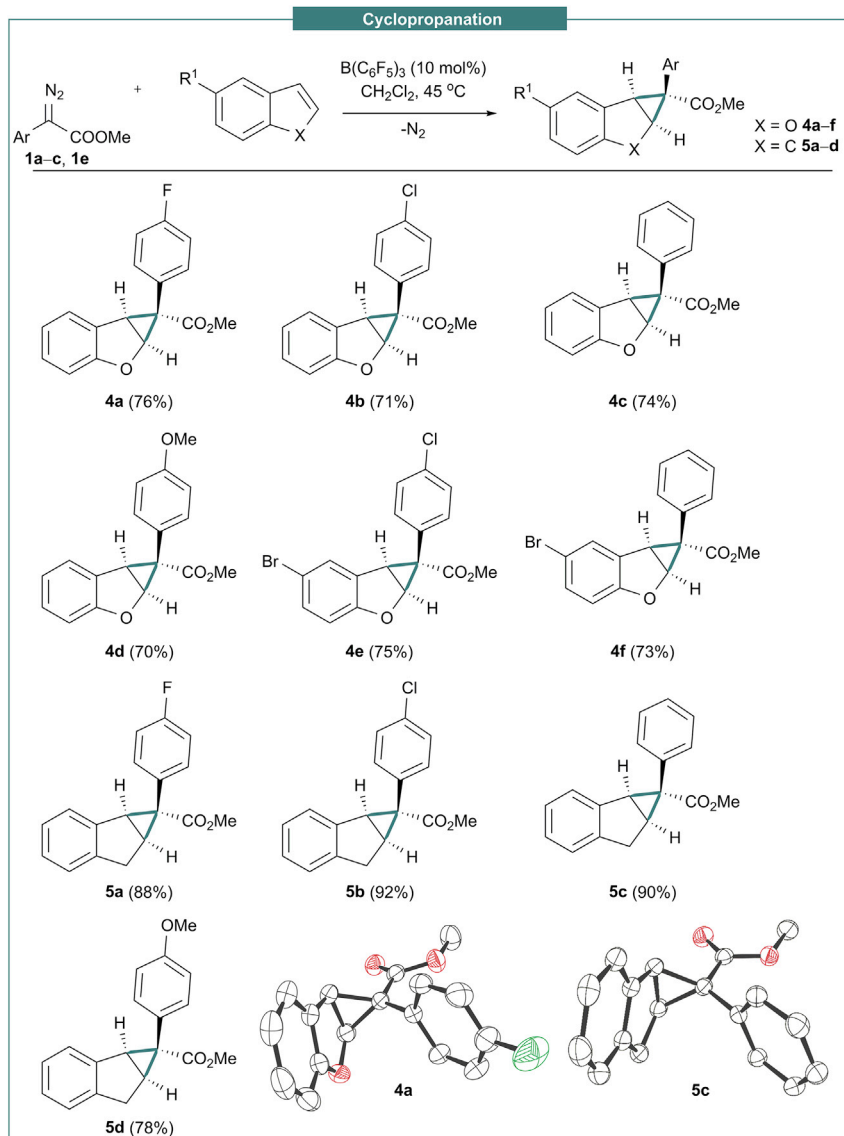
When examining the previous literature, in almost all cases, the scope has been limited to indoles where the N–H group is protected through alkylation or through the use of a protecting group.<sup>33</sup> Indeed, when metal catalysts such as rhodium are used, then additional insertion into the N–H bond is often observed as an undesired side reaction. One example where this has been overcome was reported in 2018 through the use of an engineered variant of myoglobin biocatalysts.<sup>34</sup> We therefore turned our attention to the reactivity of unprotected indoles with  $\alpha$ -aryl  $\alpha$ -diazoesters **1a–e**. Formation of the desired products **2u–y** was observed with very good isolated yields of 60%–72% (Scheme 2; Figures S56–S66). Interestingly, this reaction was

proved highly regio- and chemoselective with no N–H insertion being observed. This borane could therefore serve as an alternative to metal catalysts for the selective C–H insertion in the presence of an N–H group. This can reduce the number of steps in chemical synthesis due to the reduced need to protect and deprotect the N-atom. Suitable single crystals for X-ray diffraction of the products **2f** and **2w** were afforded from the slow evaporation of a saturated CH<sub>2</sub>Cl<sub>2</sub> solution at room temperature, confirming the structures of these products (Scheme 2, bottom; Figures S152 and S153; Tables S2 and S3). When pyrroles were investigated in this reaction, C–H insertion was also observed generating alkylation products as observed with transition metal carbenoids.<sup>35</sup> This time, exclusive C2-insertion resulted, consistent with typical electrophilic substitution reactions of pyrroles.<sup>36</sup> **3a** and **3b** were generated in 65% and 68% yields, respectively, when **1c** and **1e** were reacted with *N*-methylpyrrole (Scheme 2; Figures S77–S80). If the C2 position is blocked, then very little reaction takes place, leaving the starting pyrrole as the major species in solution.

The encouraging outcome from the reactions of *N*-heterocycles with  $\alpha$ -aryl  $\alpha$ -diazooesters increased our curiosity to investigate the borane-catalyzed reactions with other (hetero) cycles including benzofurans and indenenes. Again, B(C<sub>6</sub>F<sub>5</sub>)<sub>3</sub> (10 mol %) was found to be the best catalyst for these reactions with a single product being isolated after 20 h at 45°C. The crude <sup>1</sup>H NMR spectrum of the reaction of **1a** with 2,3-benzofuran displayed two doublets at  $\delta = 5.34$  ppm and  $\delta = 3.79$  ppm, indicating that the carbene had added into the C2, C3 double bond of the benzofuran generating the cyclopropanated product (Scheme 3). Cyclopropanes are key motifs in biologically active compounds with antibiotic, antimicrobial, antitumor, or antiviral activities.<sup>37</sup> As above, the most common way to make such compounds is the transfer of a carbene from a diazocarbonyl compound (usually via a rhodium-carbenoid intermediate) to an olefin.<sup>38</sup> Yet, intermolecular diastereoselective cyclopropanation remains a challenge.<sup>39</sup> Using the same optimized reaction conditions, 2,3-benzofuran and 5-bromobenzofuran were tested for the reaction with  $\alpha$ -aryl  $\alpha$ -diazooesters **1** (Scheme 3). The products **4a–f** were isolated as a single diastereoisomer in good yields (70%–76%, Scheme 3; Figures S81–S93). Indene also underwent diastereoselective cyclopropanation with **1a–c** and **1e** yielding the products **5a–d** in 78%–92% yield (Scheme 3; Figures S94–S102). Slow evaporation of a saturated solution of products **4a** and **5c** from CH<sub>2</sub>Cl<sub>2</sub> afforded single crystals of the product, which were measured by X-ray diffraction unambiguously confirming the structure and diastereoselectivity of the reaction (Scheme 3; Figures S154 and S155; Tables S4 and S5).

In addition to cyclopropanation of benzofurans and indene, we also trialed the cyclopropanation of other olefins (Scheme 4). Initially, styrene was reacted with **1a**, **1b**, and **1e** under the same conditions described above. Of note, the products were obtained as a single diastereoisomer **6a–c** in 81%, 83%, and 70% isolated yields, respectively (Scheme 4; Figures S103–S109 and S123–S125). Other 1-substituted olefins also worked with 2-vinylnaphthalene, giving the product **6d** in 78% yield (Figures S110, S111, and S126) when reacted with **1b**. Both 1,1-disubstituted (terminal) and 1,2-disubstituted (internal) olefins were also successful giving the products **6e–h** in 71%–77% yield (Scheme 4; Figures S112–S120, S127, and S128). Again, the 1,2-disubstituted olefins displayed highly diastereoselective reactions. Importantly, when trimethyl((2-vinylphenyl)ethynyl)silane was employed, we observed exclusive reactivity at the alkene functionality and not the alkyne giving **6i** (Figures S121, S122, and S129) in 79% yield as a single diastereoisomer. Limitations of this reaction were the non-aromatic cyclic olefins including cyclohexene and limonene.

Considering the differing selectivity between the C–H insertion product obtained for indoles versus cyclopropanation products for indenenes and benzofuran, we decided

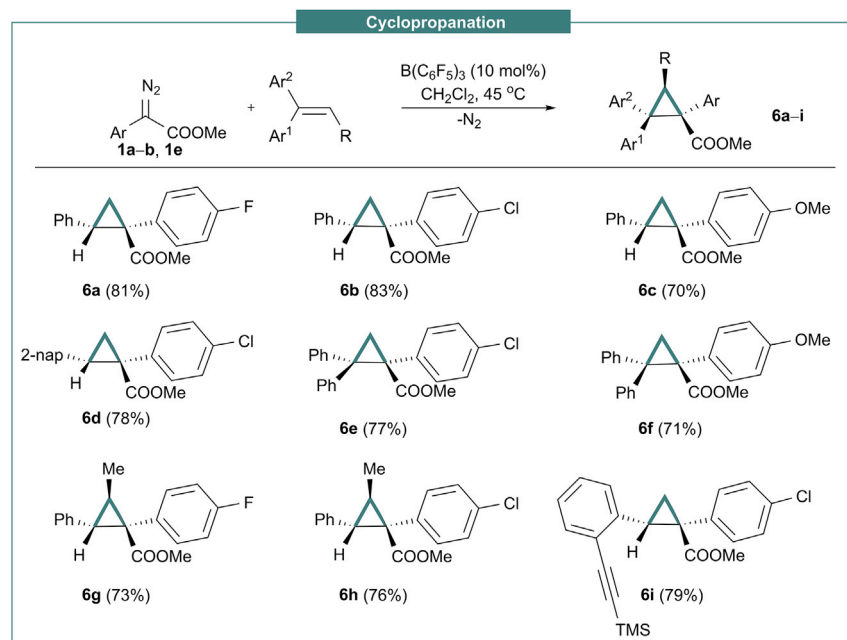


### Scheme 3. Catalytic Cyclopropanation of Benzofurans and Indenes Using $B(C_6F_5)_3$

Conditions: diazoester (1 equiv), benzofuran/indene (1.1 equiv), and  $B(C_6F_5)_3$  (10 mol %) in  $CH_2Cl_2$  (1.5 mL) at  $45^\circ C$ . All the yields reported are isolated yields. Bottom right: solid-state structures of 4a (left) and 5c (right). Thermal ellipsoids are drawn at 50% probability. H atoms omitted for clarity.

to undertake several competition experiments to investigate the comparative rates of reactions and selectivity between the different substrates (Figure S151). Using the optimized reaction condition we performed three competition reactions (Scheme 5) using equimolar mixture of (1) 1-methylindole and 2,3-benzofuran, (2) 1-methylindole and 1*H*-indene, and (3) 2,3-benzofuran and 1*H*-indene with 1 equiv of diazo compound 1b and 10 mol %  $B(C_6F_5)_3$ . The progress of the reactions was monitored by  $^1H$  NMR spectroscopy using mesitylene as an internal standard. Interestingly, when indole was present, the exclusive formation of the C3 C–H insertion product (2b) was observed showing 89% and 88% conversion after 22 h. In these cases, the benzofuran and indene substrates remained untouched, showing no cyclopropanation products 4b and 5b, respectively. These results indicate that the indole is far more reactive (nucleophilic) than the benzofuran and indene substrates.



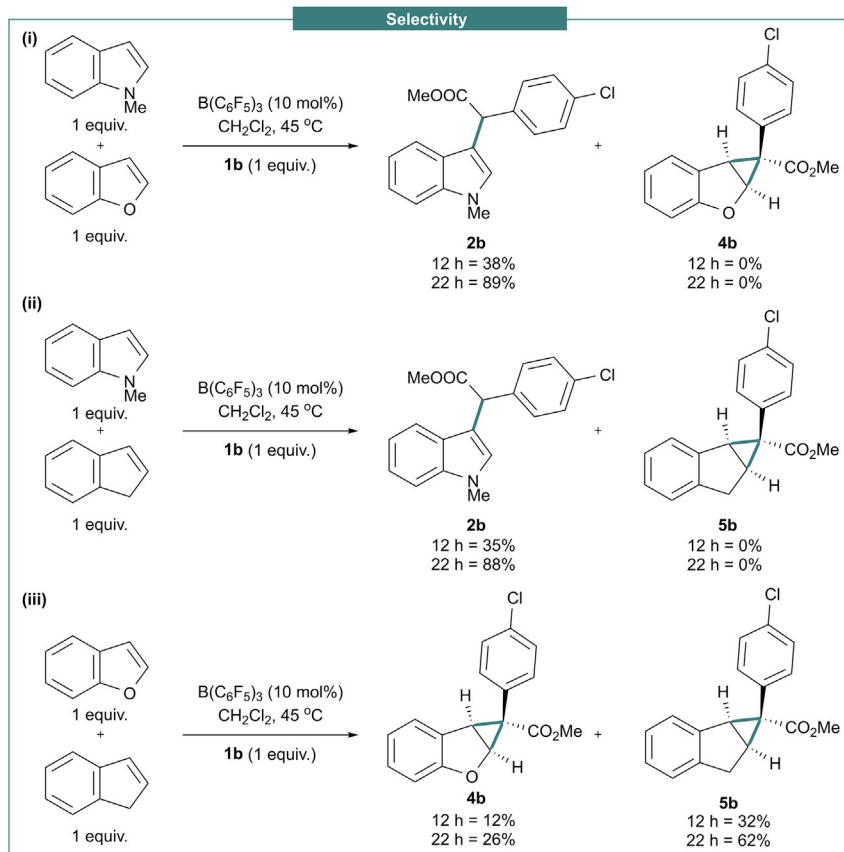


**Scheme 4. Catalytic Cyclopropanation of Olefins Using  $B(C_6F_5)_3$**

Conditions: diazoester (1 equiv), olefin (1.1 equiv), and  $B(C_6F_5)_3$  (10 mol %) in  $CH_2Cl_2$  (1.5 mL) at  $45^\circ C$ . All the yields reported are isolated yields.

Alternatively, when equimolar mixture of 2,3-benzofuran and 1*H*-indene were reacted with **1b**, formation of both the cyclopropanation products **4b** and **5b** were observed. In these cases, indene reacts faster than benzofuran, showing a 1:2.9 ratio of **4b**:**5b** after 22 h.

Finally, we turned our attention to the borane-catalyzed reactions of  $\alpha$ -aryl  $\alpha$ -diazoesters with furan substrates. Indeed, the synthesis and subsequent transformations of furans is an important area of research.<sup>40</sup> Recently, they have received attention in the area of renewable biomass where the acid-catalyzed thermal dehydration of sugars provides furan compounds, which may be used as convenient starting materials in organic synthesis.<sup>41</sup> Compared with reactions that involve functionalization of the furan heterocycle keeping the five membered ring intact, ring-opening reactions have been less studied<sup>42</sup> although recently  $B(C_6F_5)_3$  was shown to be an excellent catalyst for the tandem ring-opening and hydrosilylation of furans to obtain silicon-functionalized products.<sup>43</sup> We therefore sought to investigate the tandem borane-catalyzed carbene transfer and ring-opening reactions of furans. Initially, **1a** was reacted with furan in the presence of a Lewis acidic borane catalyst (10 mol %) generating a single ring-opened product **7a** (Scheme 6; Figures S130–S132). Again, reaction optimization showed that mild conditions ( $45^\circ C$  in  $CH_2Cl_2$ ) were needed for the reaction to complete, but in this case, the less Lewis acidic borane 2,4,6-trifluorophenylborane [ $B(2,4,6-F_3C_6H_2)_3$ ] was found to be a better catalyst than  $B(C_6F_5)_3$ , giving 61% yield of the product **7a** compared with 52%. We then extended the scope of the reaction to 2-methylfuran and 2,5-dimethylfuran with  $\alpha$ -aryl  $\alpha$ -diazoesters **1** to generate the products **7b–i** in 64%–82% yields (Scheme 6; Figures S133–S150). In all cases, just a single diastereoisomer was generated, which could also be confirmed by single-crystal X-ray diffraction analysis for compounds **7a** and **7h** (Scheme 6, bottom, Figures S156 and S157; Tables S6 and S7).

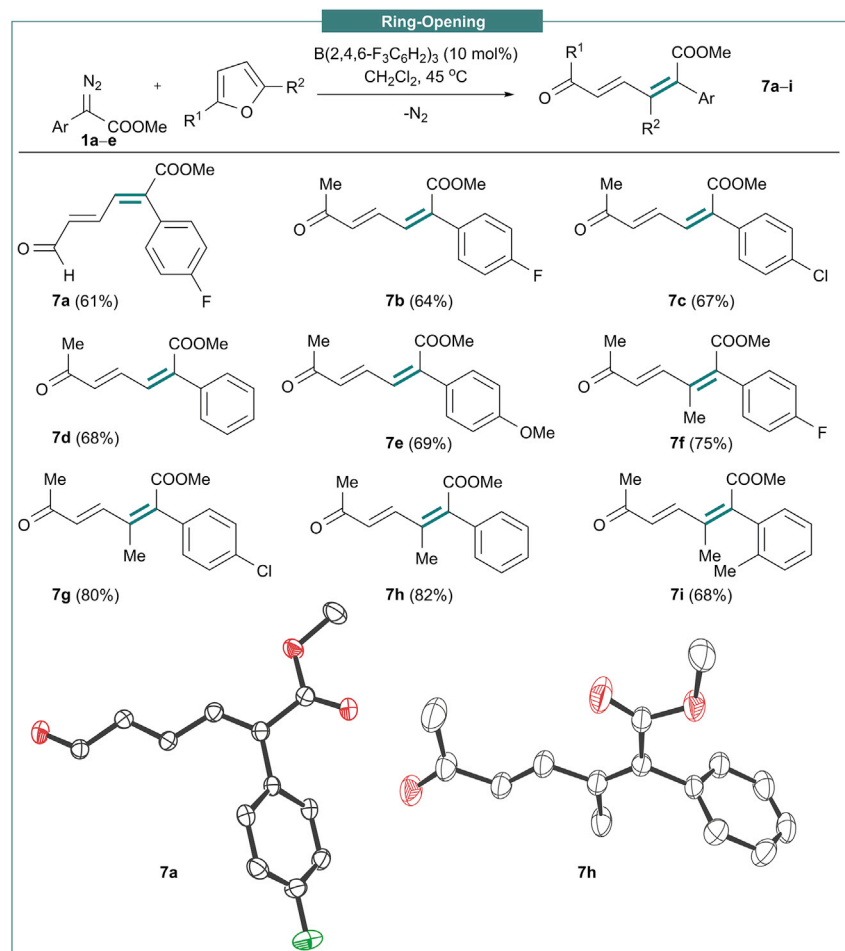


### Scheme 5. Competition Reactions between Indole, Benzofuran, and Indene

Conditions: diazoester **1b** (1 equiv.), (hetero)cycle (1 equiv each), and  $\text{B}(\text{C}_6\text{F}_5)_3$  (10 mol %) in  $\text{CH}_2\text{Cl}_2$  (1.5 mL) at  $45^\circ\text{C}$ . All the yields reported are NMR yields using mesitylene as an internal standard.

### Computational Studies

To examine the contrasting products obtained for indole, indene, benzofuran, styrene, pyrrole, and furan-based moieties, we undertook a thorough DFT investigation of all the potential reaction pathways. We focused upon the driving force for the C–H insertion product obtained for pyrroles and indoles versus the cyclopropanation products for styrenes, indenenes, and benzofurans versus the ring-opened products for furans. Calculations were performed at the SMD/M06-2X-D3/def2-TZVP//CPCM/B3LYP/6-31G(d) level of theory to examine the origin of the contrasting products (Tables S8–S63). Regardless of the substrate, the first step in the reaction is the same, namely  $\text{B}(\text{C}_6\text{F}_5)_3$  activation of the diazo reagent (Scheme 7, see Figure S158 for the free energy profile). It transpires that formation of species **I2** (Scheme 7) is a prerequisite for all pathways. This can be obtained when  $\text{B}(\text{C}_6\text{F}_5)_3$  binds effectively with the carbonyl oxygen atom of the diazoester starting material **1** to form intermediate **I1**, as seen in our previous studies.<sup>21</sup> The  $\text{B}(\text{C}_6\text{F}_5)_3$  coordination results in the C–N bond in **I1** becoming weaker than that in starting material **1**, thereby making  $\text{N}_2$  a better leaving group. The weakening of the C–N bond is ascribed to the increased contribution of the resonance structure **I1'**, as evidenced by the lengthening of the C–N bond (1.334 Å in **I1** versus 1.318 Å in **1**) as well as the shortening of the C–C bond (1.436 Å in **I1** versus 1.470 Å in **1**) (see Figure S158). This facilitates the release of  $\text{N}_2$ , yielding the key species **I2** with an energy barrier of 25 kcal/mol ( $\text{TS}_2$  in Figure S158).<sup>29</sup> Two resonance structures of **I2** (**I2'** and **I2''**) describe the structure and

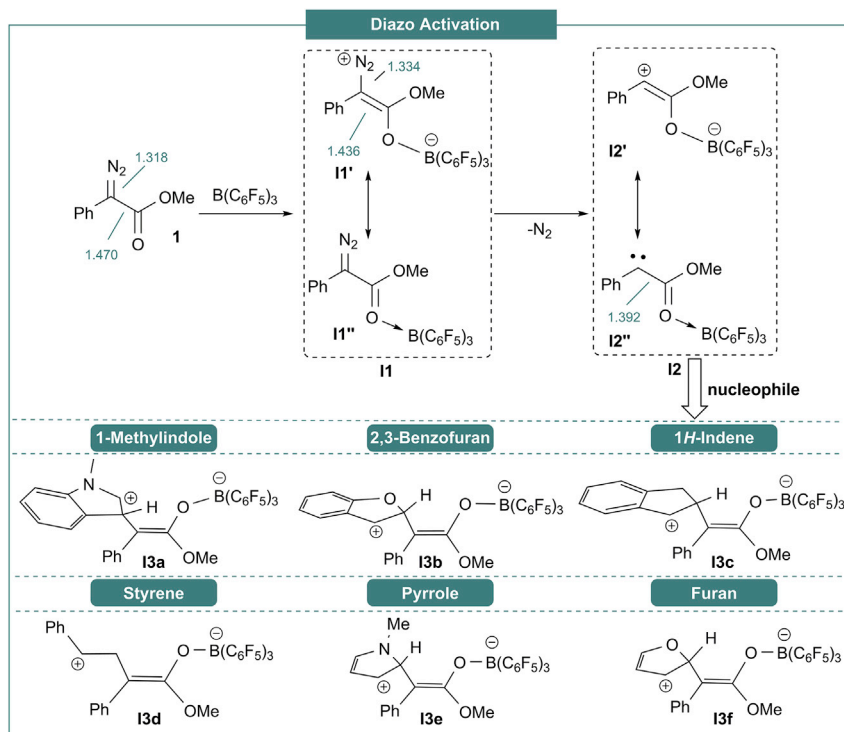


### Scheme 6. Catalytic Ring-Opening of Furans

Conditions: diazoester (1 equiv), furan (1.1 equiv), and B(2,4,6-F<sub>3</sub>C<sub>6</sub>H<sub>2</sub>)<sub>3</sub> (10 mol %) in CH<sub>2</sub>Cl<sub>2</sub> (1.5 mL) at 45 °C. All the yields reported are isolated yields. Bottom: solid-state structures of **7a** (left) and **7h** (right). Thermal ellipsoids drawn at 50% probability. H atoms omitted for clarity.

bonding of this key intermediate. This is confirmed by the fact that the C–C bond in **I2** (1.392 Å) is significantly shorter than that in **I1** (1.436 Å) and starting diazo compound **1** (1.470 Å). Furthermore, species **I2** is highly electron deficient, leading to its ability to readily react with nucleophiles in an appreciably exergonic fashion giving intermediates **I3a–f** (Scheme 7), which then proceed to generate the C–H insertion, cyclopropanated, or ring-opened products. Owing to the electron-deficient nature of **I2**, any transition structure for the addition of (hetero)cycles to **I2** was difficult to locate. It should be noted that attempts to locate an associative transition structure in which a (hetero)cycle serves as a nucleophile and attacks intermediate **I1** were unsuccessful. On the basis of our calculations, this step is energetically highly favorable, a result which is in agreement with the previous reports by Wu et al.<sup>29</sup>

At the heart of the contradistinct reactivity between the different nucleophiles is the competition between forming the cyclopropanation product (**P1**) versus the C–H insertion product (**P2**), or the ring-opened product (**P3**). Once intermediate **I3** (Scheme 7) is formed, it is the branching point for the three different processes: (1) C–H insertion, (2) ring-opening, and (3) cyclopropanation. The nature of the



**Scheme 7.** DFT-Calculated Activation of Diazo Substrates by  $B(C_6F_5)_3$

Bond lengths measured in Å.

(hetero)cycles plays the most important role as to which pathway is taken. For all (hetero)cycles, the cyclopropanation occurs with a much lower barrier than the other two pathways. This suggests that the cyclopropanated species should be the first

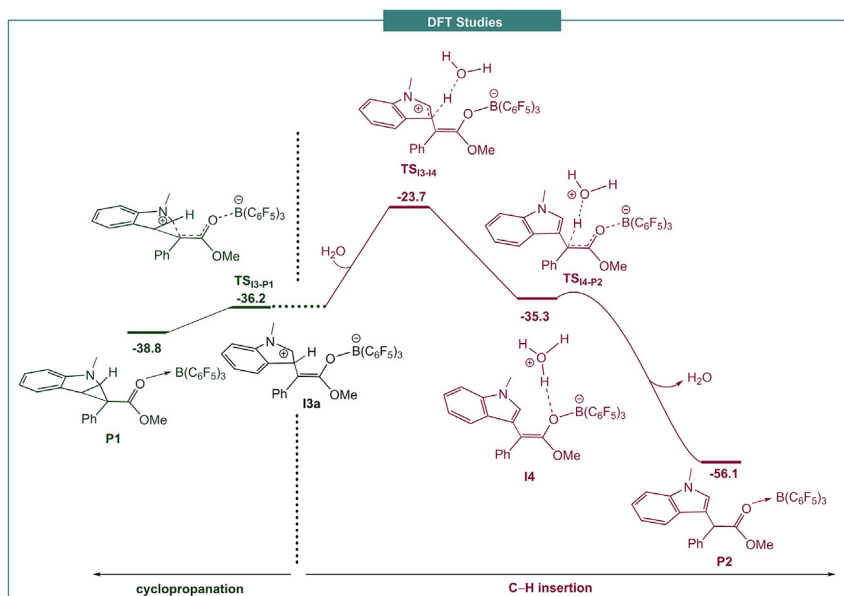


**Figure 1.** DFT Computed Reaction Pathways for the Reaction of Indole Substrates with Diazoesters and  $B(C_6F_5)_3$

The relative free energies are given in kcal/mol.



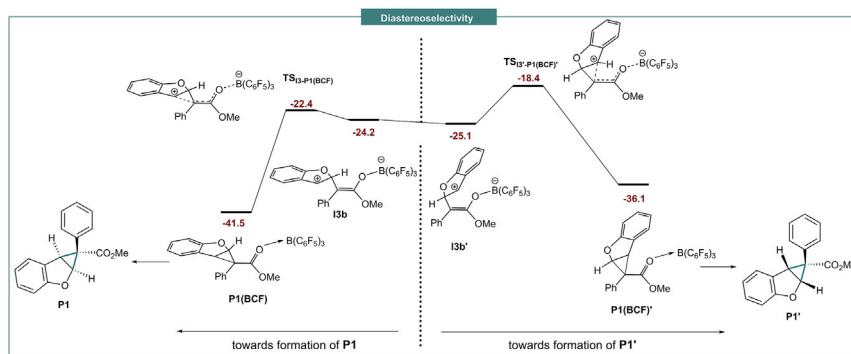


**Figure 3. Energy Profiles for the Different Diastereoisomers of the Reaction**

Computed reaction pathways for the two possible diastereoisomers for the reaction of diazoesters with benzofuran-catalyzed  $B(C_6F_5)_3$ . The relative free energies are given in kcal/mol.

ring-opening (Figure 2). In this case, the first kinetic cyclopropanated product **P1** is so stable that it does not allow the thermodynamic C–H insertion product **P2** to be formed under the reaction conditions; starting from the cyclopropanated product **P1**, formation of the thermodynamic C–H insertion product **P2** would need to cross a very high barrier of 32.6 kcal/mol. Similar to indoles, benzofuran is also unreactive toward the ring-opening process because of the disruption of the aromaticity of the six-membered ring in the ring-opened product **P3**. The same result is observed for indene and styrene substrates (see Figures S160 and S161) in that the reaction between the indene or styrene nucleophiles with **I2** immediately gives the kinetic cyclopropanated product **P1** (Figure S163). As with benzofuran, these kinetic products are too stable to undergo the reverse transformation to afford the thermodynamic C–H insertion product **P2**.

We also undertook calculations to explain our observed diastereoselectivity for the cyclopropanation reactions with benzofurans, indenenes, and styrenes. Using benzofuran as an example, we found that  $TS_{13-P1(BCF)}$  lies 4.0 kcal/mol lower in energy than  $TS_{13-P1'(BCF)'}$  and that **P1** is thermodynamically more stable than **P1'** (Figure 3). This is presumably because of the reduced steric hindrance in  $TS_{13-P1(BCF)}$  brought about by the sterically demanding  $B(C_6F_5)_3$  moiety.

Finally, we turned our attention to explaining the contradistinct reactivity of the 5-membered heterocycles pyrrole and furan that give the C2 C–H insertion and ring-opened products, respectively. For pyrrole, the energy profile (Figure 4, top) related to competition between the three pathways indicates that although the pathways leading to cyclopropanated **P1** and ring-opening products **P3** are kinetically favored over the C–H insertion pathway, they are not stable thermodynamically; both **P1** and **P3** energetically lie above **I3e**. In contrast, the C–H insertion pathway starting from **I3e** assisted by an adventitious water molecule by surmounting an activation barrier of 22.8 kcal/mol gives **P2** with  $\Delta G_{rxn} = -17.5$  kcal/mol. The calculations predict that the presence of an adventitious water molecule is required as a catalyst for the C–H insertion pathway to occur with an accessible activation barrier. The direct proton transfers are found to be more energy demanding with  $\Delta G^\ddagger > 30$  kcal/mol (see Figure S162). Finally, we calculated the three possible pathways for the case of furan (Figure 4, bottom). For this heterocycle, the first kinetic product (cyclopropanation, **P1**) is about 7.7 kcal/mol higher in energy than the second kinetic product (ring-opening, **P3**), and thus, the former can be converted to the latter through a reverse transformation by overcoming an

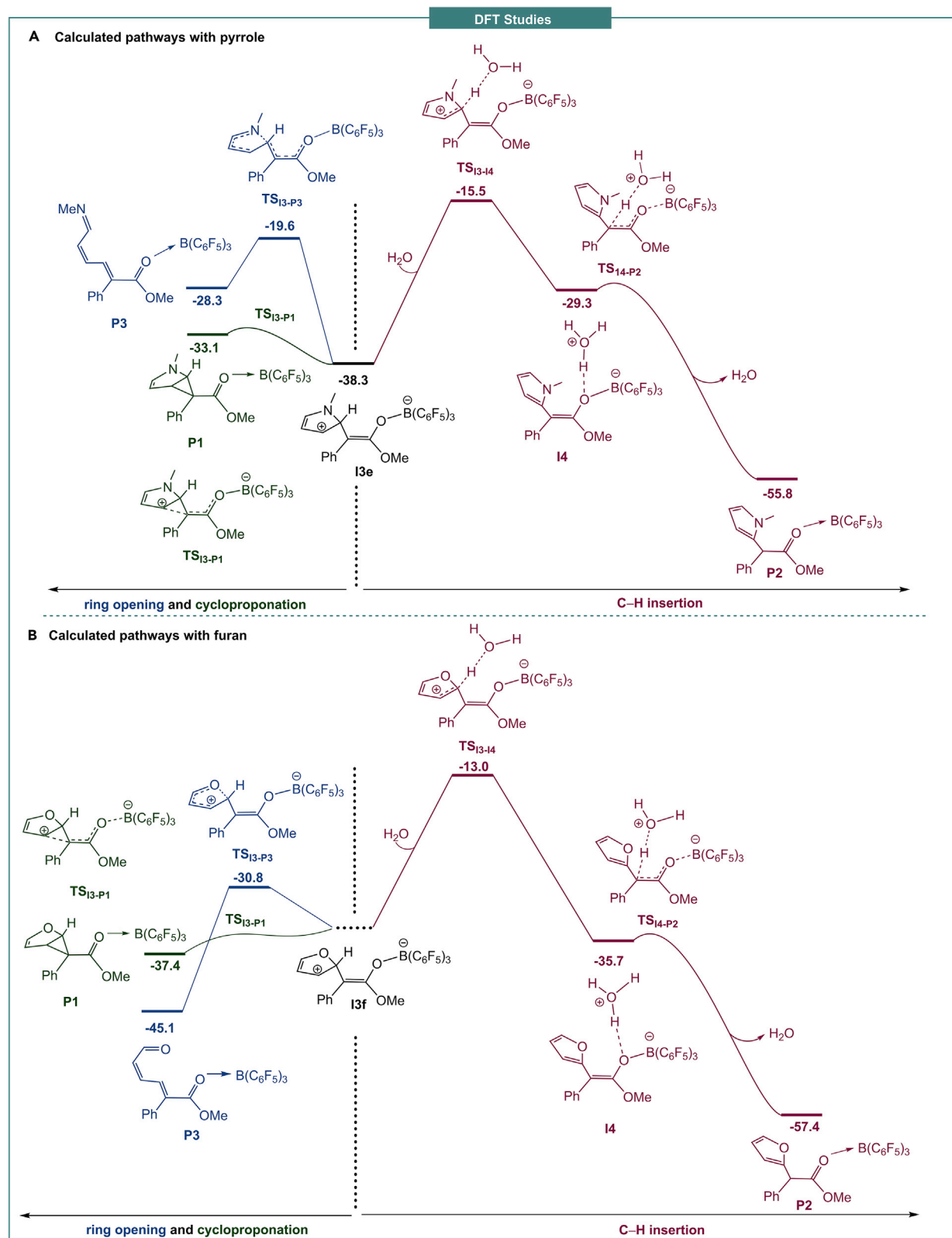


**Figure 4. DFT Computed Reaction Pathways for Pyrrole and Furan Substrates with Diazoesters and  $B(C_6F_5)_3$**

The reaction of pyrrole substrates (top) and furan substrates (bottom). The relative free energies are given in kcal/mol.

activation free energy of 6.6 kcal/mol (energy difference between P1 and TS<sub>13-P3</sub>). In this case, formation of the thermodynamic C–H insertion product P2 requires surmounting a free energy barrier of 32.1 kcal/mol (energy difference between P3 and TS<sub>13-14</sub>), which is too high to be attainable under the reaction conditions. This result rationalizes why for furan, only the ring-opening product is experimentally observed. Furan is more reactive than pyrrole toward ring-opening, likely due to a higher preference for a carbon atom to form a  $\pi$ -bond with oxygen than with a nitrogen atom in the reaction.

### Conclusions

In conclusion, we have shown that Lewis-acidic-fluorinated triarylboranes can be used as effective metal-free catalysts for highly selective reactions of donor-acceptor diazo compounds to a range of substrates. The reactions of  $\alpha$ -aryl  $\alpha$ -diazoesters with the nitrogen heterocycles indole or pyrrole selectively generate the C3 and C2 C–H insertion products, respectively, in good to excellent yields even when using unprotected indoles. Alternatively, benzofuran, indene, and olefin substrates give exclusively the cyclopropanated products with  $\alpha$ -aryl  $\alpha$ -diazoesters, whereas the reactions with furans lead to ring-opening with C=C bond formation. DFT calculations have been employed to understand the reaction mechanisms as well as the differing regio- and diastereoselectivities of the substrates. Overall, this work demonstrates the highly selective metal-free catalytic reactions of  $\alpha$ -aryl  $\alpha$ -diazoesters with a range of (hetero)cycles and olefins. This simple, mild reaction protocol represents an alternative to the commonly used precious metal systems and may provide future applications in the generation of biologically active compounds.

## EXPERIMENTAL PROCEDURES

### Resource Availability

#### Lead Contact

Further information and requests for resources and reagents should be directed to and will be fulfilled by the Lead Contact, Rebecca Melen ([MelenR@cardiff.ac.uk](mailto:MelenR@cardiff.ac.uk)).

#### Materials Availability

Unique and stable reagents generated in this study will be made available on request, but we may require a payment and/or a completed Materials Transfer Agreement if there is potential for commercial application.

#### Data and Code Availability

Crystallographic data for 2f, 2w, 4a, 5c, 7a, and 7h have been deposited in the Cambridge Crystallographic Data Center (CCDC) under accession numbers CCDC: 1940993, 1939757, 1939753, 1939756, 1939754, and 1939755. These data can be obtained free of charge from the CCDC at [http://www.ccdc.cam.ac.uk/data\\_request/cif](http://www.ccdc.cam.ac.uk/data_request/cif). Information about the data that underpins the results presented in this article, including how to access them, can be found in the Cardiff University data catalog at <http://doi.org/10.17035/d.2020.0111365980>. All other data are available from the Lead Contact upon reasonable request.

### Representative Procedure for Boron-Catalyzed Reactions

Under a nitrogen atmosphere, the triarylborane (10 mol %) was dissolved in CH<sub>2</sub>Cl<sub>2</sub> (0.5 mL) and added to a CH<sub>2</sub>Cl<sub>2</sub> solution (0.5 mL) of diazoester 1 (0.2 mmol, 1 equiv). The heteroarene/indene/alkene substrate (0.22 mmol, 1.1 equiv) in CH<sub>2</sub>Cl<sub>2</sub> (0.5 mL) was then added to the reaction mixture dropwise. The reaction was heated at 45°C for 18–24 h before all volatiles were removed *in vacuo* and the crude compound



purified via column chromatography on silica using hexane/ethyl acetate as eluent. Full experimental procedures are provided in the [Supplemental Information](#).

## SUPPLEMENTAL INFORMATION

Supplemental Information can be found online at <https://doi.org/10.1016/j.chempr.2020.06.035>.

## ACKNOWLEDGMENTS

We are grateful to the EPSRC (B.S., EP/L000202) and (A.D., EP/R026912/1) for funding and the awarding of an EPSRC Early Career Fellowship (R.L.M., EP/R026912/1). A.A., B.F.Y., and R.B. thank the Australian Research Council (ARC) for project funding (DP180100904) and the Australian National Computational Infrastructure and the University of Tasmania for the generous allocation of computing time. The authors would also like to acknowledge Dasara Hadri for performing preliminary calculations into the reaction mechanisms.

## AUTHOR CONTRIBUTIONS

A.D. designed the project and performed all of the experimental work. R.B., B.F.Y., B.S., and A.A. undertook all the DFT calculations. R.L.M. directed the project. R.L.M. wrote the manuscript with input from all authors. All authors analyzed the results and commented on the manuscript.

## DECLARATION OF INTERESTS

The authors declare no competing interests.

Received: February 24, 2020

Revised: May 22, 2020

Accepted: June 25, 2020

Published: July 22, 2020

## REFERENCES

1. For reviews, see: Roh, S.W., Choi, K., and Lee, C. (2019). Transition metal vinylidene- and allenylidene-mediated catalysis in organic synthesis. *Chem. Rev.* 119, 4293–4356. Xia, Y., Qiu, D., and Wang, J. (2017). Transition-metal-catalyzed cross-couplings through carbene migratory insertion. *Chem. Rev.* 117, 13810–13889. Schubert, U. (1984). Structural consequences of bonding in transition metal carbene complexes. *Coord. Chem. Rev.* 55, 261–286. Cardin, D.J., Cetinkaya, B., and Lappert, M.F. (1972). Transition metal-carbene complexes. *Chem. Rev.* 72, 545–574. Also see: Barluenga, J., Rodríguez, F., Fañanás, F.J., and Flórez, J. (2004). In *Metal Carbenes in Organic Synthesis*. Topics in Organometallic Chemistry, K.H. Dötz, ed. (Springer), pp. 59–122.
2. For reviews, see: Wencel-Delord, J., and Glorius, F. (2013). C–H bond activation enables the rapid construction and late-stage diversification of functional molecules. *Nat. Chem.* 5, 369–375. Bandini, M., and Eichholzer, A. (2009). Catalytic functionalization of indoles in a new dimension. *Angew. Chem. Int. Ed.* 48, 9608–9644. For recent examples, see: Ye, Y., Kim, S.T., Jeong, J., Baik, M.H., and Buchwald, S.L. (2019). CuH-catalyzed enantioselective alkylation of indole derivatives with ligand-controlled regio divergence. *J. Am. Chem. Soc.* 141, 3901–3909. Qiu, X., Deng, H., Zhao, Y., and Shi, Z. (2018). Rhodium-catalyzed, P-directed selective C7 arylation of indoles. *Sci. Adv.* 4, eaau6468. Cheng, Q., Zhang, H.-J., Yue, W.-J., and You, S.-L. (2017). Palladium-catalyzed highly stereoselective dearomative [3 + 2] cycloaddition of nitrobenzofurans. *Chem* 3, 428–436. Zheng, C., and You, S.-L. (2016). Catalytic asymmetric dearomatization by transition-metal catalysis: a method for transformations of aromatic compounds. *Chem* 1, 830–857.
3. Xing, D., and Hu, W. (2014). Diazoacetate and related metal-stabilized carbene species in MCRs. In *Multicomponent Reactions in Organic Synthesis*, J. Zhu, Q. Wang, and M. Wang, eds. (Wiley), pp. 183–206. M.P. Doyle, M.A. McKervey, and T. Ye, eds. *Modern Catalytic Methods for Organic Synthesis with Diazo Compounds: From Cyclopropanes to Ylides* (Wiley). Maas, G. (1987). Transition-metal catalyzed decomposition of aliphatic diazo compounds—new results and applications in organic synthesis. In *Organic Synthesis, Reactions and Mechanisms*. Topics in Current Chemistry (Springer), pp. 75–253.
4. Doyle, M.P., Duffy, R., Ratnikov, M., and Zhou, L. (2010). Catalytic carbene insertion into C–H bonds. *Chem. Rev.* 110, 704–724.
5. Brookhart, M., and Studabaker, W.B. (1987). Cyclopropanes from reactions of transition-metal-carbene complexes with olefins. *Chem. Rev.* 87, 411–432.
6. Jana, S., and Koenigs, R.M. (2019). Rhodium-catalyzed carbene transfer reactions for sigmatropic rearrangement reactions of selenium ylides. *Org. Lett.* 21, 3653–3657. Xu, X., Hu, W.H., Zavalij, P.Y., and Doyle, M.P. (2011). Divergent outcomes of carbene transfer reactions from dirhodium- and copper-based catalysts separately or in combination. *Angew. Chem. Int. Ed.* 50, 11152–11155.
7. Xu, G., Liu, K., and Sun, J. (2018). Gold-catalyzed controllable C2-functionalization of benzofurans with aryl diazoesters. *Org. Lett.* 20, 72–75.
8. Leitch, J.A., McMullin, C.L., Mahon, M.F., Bhonoah, Y., and Frost, C.G. (2017). Remote C6-selective ruthenium-catalyzed C–H alkylation of indole derivatives via  $\sigma$ -activation. *ACS Catal.* 7, 2616–2623.
9. Yang, Z., Möller, M., and Koenigs, R.M. (2020). Synthesis of gem-difluoro olefins through C–H functionalization and  $\beta$ -fluoride elimination reactions. *Chem. Int. Ed.* 59, 5572–5576. Yang, Y., Qiu, X., Zhao, Y., Mu, Y., and Shi,

- Z. (2016). Palladium-catalyzed C–H arylation of indoles at the C7 position. *J. Am. Chem. Soc.* 138, 495–498. Kandukuri, S.R., Jiao, L.-Y., Machotta, A.B., and Oestreich, M. (2014). Diastereotopic group selection in hydroxy-directed intramolecular C–H alkenylation of indole under oxidative palladium(II) catalysis. *Adv. Synth. Catal.* 356, 1597–1609.
10. Li, M., Guo, X., Jin, W., Zheng, Q., Liu, S., and Hu, W. (2016). An enantioselective three-component reaction of diazoacetates with indoles and enals by iridium/iminium co-catalyst. *Chem. Commun.* 52, 2736–2739.
11. Fraile, J.M., Le Jeune, K., Mayoral, J.A., Ravasio, N., and Zaccheria, F. (2013). CuO/SiO<sub>2</sub> as a simple, effective and recoverable catalyst for alkylation of indole derivatives with diazo compounds. *Org. Biomol. Chem.* 11, 4327–4332.
12. Wang, B., Howard, I.G., Pope, J.W., Conte, E.D., and Deng, Y. (2019). Bis(imino)pyridine iron complexes for catalytic carbene transfer reactions. *Chem. Sci.* 10, 7958–7963. Cai, Y., Zhu, S.-F., Wang, G.-P., and Zhou, Q.-L. (2011). Iron-catalyzed C–H functionalization of indoles. *Adv. Synth. Catal.* 353, 2939–2944.
13. Jana, S., Li, F., Empel, C., Verspeek, D., Aseeva, P., and Koenigs, R.M. (2020). Stoichiometric photochemical carbene transfer reactions via Bamford Stevens reaction. *Chem. Eur. J.* 26, 2586–2591. Guo, Y., Nguyen, T.V., and Koenigs, R.M. (2019). Norcaradiene synthesis via visible-light-mediated cyclopropanation reactions of arenes. *Org. Lett.* 21, 8814–8818. Ciszewski, Ł.W., Durka, J., and Gryko, D. (2019). Photocatalytic alkylation of pyrroles and indoles with  $\alpha$  diazo esters. *Org. Lett.* 21, 7028–7032. Li, P., Zhao, J., Shi, L., Wang, J., Shi, X., and Li, F. (2018). Iodine-catalyzed diazo activation to access radical reactivity. *Nat. Commun.* 9, 1972. Jurberg, I.D., and Davies, H.M.L. (2018). Blue light-promoted photolysis of aryldiazoacetates. *Chem. Sci.* 9, 5112–5118.
14. Egorova, K.S., and Ananikov, V.P. (2017). Toxicity of metal compounds: knowledge and myths. *Organometallics* 36, 4071–4090. Zhou, Q.L. (2016). Transition-metal catalysis and organocatalysis: where can progress be expected? *Angew. Chem. Int. Ed.* 55, 5352–5353.
15. For reviews on modern main group chemistry, see: Melen, R.L. (2019). Frontiers in molecular p-block chemistry: from structure to reactivity. *Science* 363, 479–484. Weetman, C., and Inoue, S. (2018). The road travelled: after main-group elements as transition metals. *ChemCatChem* 10, 4213–4228. Power, P.P. (2010). Main-group elements as transition metals. *Nature* 463, 171–177. Also see: Légaré, M.A., Courtemanche, M.A., Rochette, É., and Fontaine, F.G. (2015). Boron catalysis. Metal-free catalytic C–H bond activation and borylation of heteroarenes. *Science* 349, 513–516.
16. Parks, D.J., and Piers, W.E. (1996). Tris(pentafluorophenyl)boron-catalyzed hydrosilylation of aromatic aldehydes, ketones, and esters. *J. Am. Chem. Soc.* 118, 9440–9441.
17. For a recent review, see: Stephan, D.W. (2016). The broadening reach of frustrated Lewis pair chemistry. *Science* 354, aaf7229.
18. Li, L., Wu, Z., Zhu, H., Robinson, G.H., Xie, Y., and Schaefer, H.F. (2020). Reduction of dinitrogen via 2,3'-bipyridine-mediated tetraboration. *J. Am. Chem. Soc.* 142, 6244–6250. Ruddy, A.J., Ould, D.M.C., Newman, P.D., and Melen, R.L. (2018). Push and pull: the potential role of boron in N<sub>2</sub> activation. *Dalton Trans.* 47, 10377–10381.
19. Légaré, M.A., Rang, M., Bélanger-Chabot, G., Schweizer, J.I., Krummenacher, I., Bertermann, R., Arrowsmith, M., Holthausen, M.C., and Braunschweig, H. (2019). The reductive coupling of dinitrogen. *Science* 363, 1329–1332. Légaré, M.A., Bélanger-Chabot, G., Dewhurst, R.D., Welz, E., Krummenacher, I., Engels, B., and Braunschweig, H. (2018). Nitrogen fixation and reduction at boron. *Science* 359, 896–900.
20. Geri, J.B., Shanahan, J.P., and Szymczak, N.K. (2017). Testing the push–pull hypothesis: Lewis acid augmented N<sub>2</sub> activation at iron. *J. Am. Chem. Soc.* 139, 5952–5956. Simonneau, A., Turrel, R., Vendier, L., and Etienne, M. (2017). Group 6 transition-metal/boron frustrated Lewis pair templates activate N<sub>2</sub> and allow its facile borylation and silylation. *Angew. Chem. Int. Ed.* 56, 12268–12272.
21. Santi, M., Ould, D.M.C., Wenz, J., Soltani, Y., Melen, R.L., and Wirth, T. (2019). Metal-free tandem rearrangement/lactonization: access to 3,3-disubstituted benzofuran-2-(3H)-ones. *Angew. Chem. Int. Ed.* 58, 7861–7865.
22. Neu, R.C., Jiang, C., and Stephan, D.W. (2013). Bulky derivatives of boranes, boronic acids and boronate esters via reaction with diazomethanes. *Dalton Trans.* 42, 726–736. Neu, R.C., and Stephan, D.W. (2012). Insertion reactions of diazomethanes and electrophilic boranes. *Organometallics* 31, 46–49.
23. For selected examples, see: Hooz, J., Oudenes, J., Roberts, J.L., and Benderly, A. (1987). A new regioselective synthesis of enol boranes of methyl ketones. *J. Org. Chem.* 52, 1347–1349. Hooz, J., Bridson, J.N., Calzada, J.G., Brown, H.C., Midland, M.M., and Levy, A.B. (1973). Reaction of alkyl- and aryl-dichloroboranes with ethyl diazoacetate at low temperature. *J. Org. Chem.* 38, 2574–2576. Hooz, J., and Bridson, J.N. (1973). Method for the regioselective synthesis of Mannich bases. Reaction of enol borinates with dimethyl(methylene) ammonium iodide. *J. Am. Chem. Soc.* 95, 602–603. Hooz, J., and Linke, S. (1968). The reaction of trialkylboranes with diazoacetone. A new ketone synthesis. *J. Am. Chem. Soc.* 90, 5936–5937.
24. Yu, Z., Li, Y.S., Ma, J., Liu, B.L., and Zhang, J. (2016). (C<sub>6</sub>F<sub>5</sub>)<sub>3</sub>B catalyzed chemoselective and ortho-selective substitution of phenols with  $\alpha$ -aryl  $\alpha$ -diazoesters. *Angew. Chem. Int. Ed.* 55, 14807–14811.
25. San, H.H., Wang, S.J., Jiang, M., and Tang, X.Y. (2018). Boron-catalyzed O–H bond insertion of  $\alpha$ -aryl  $\alpha$ -diazoesters in water. *Org. Lett.* 20, 4672–4676.
26. San, H.H., Wang, C.Y., Zeng, H.P., Fu, S.T., Jiang, M., and Tang, X.Y. (2019). Boron-catalyzed azide insertion of  $\alpha$ -aryl  $\alpha$ -diazoesters. *J. Org. Chem.* 84, 4478–4485.
27. Rao, S., Kapaniaiah, R., and Prabhu, K.R. (2019). Boron-catalyzed C–C functionalization of allyl alcohols. *Adv. Synth. Catal.* 361, 1301–1306.
28. Tang, C., Liang, Q., Jupp, A.R., Johnstone, T.C., Neu, R.C., Song, D., Grimme, S., and Stephan, D.W. (2017). 1,1-Hydroboration and a borane adduct of diphenyldiazomethane: a potential prelude to FLP–N<sub>2</sub> chemistry. *Angew. Chem. Int. Ed.* 56, 16588–16592. Also see: Melen, R.L. (2018). A step closer to metal-free dinitrogen activation: a new chapter in the chemistry of frustrated Lewis pairs. *Angew. Chem. Int. Ed.* 57, 880–882.
29. Zhang, Q., Zhang, X.F., Li, M., Li, C., Liu, J.Q., Jiang, Y.Y., Ji, X., Liu, L., and Wu, Y.C. (2019). Mechanistic insights into the chemo- and regio-selective B(C<sub>6</sub>F<sub>5</sub>)<sub>3</sub> catalyzed C–H functionalization of phenols with diazoesters. *J. Org. Chem.* 84, 14508–14519.
30. Hao, J., Xu, Y., Xu, Z., Zhang, Z., and Yang, W. (2018). Pd-catalyzed three-component Domino reaction of vinyl benzoxazinones for regioselective and stereoselective synthesis of allylic sulfone-containing amino acid derivatives. *Org. Lett.* 20, 7888–7892.
31. For reviews, see: Zhang, M.Z., Chen, Q., and Yang, G.F. (2015). A review on recent developments of indole-containing antiviral agents. *Eur. J. Med. Chem.* 89, 421–441. Kochanowska-Karamyan, A.J., and Hamann, M.T. (2010). Marine indole alkaloids: potential new drug leads for the control of depression and anxiety. *Chem. Rev.* 110, 4489–4497. For selected examples, see: Zou, Y., and Smith, A.B. (2018). Total synthesis of architecturally complex indole terpenoids: strategic and tactical evolution. *J. Antibiot.* 71, 185–204. Yap, W.S., Gan, C.Y., Low, Y.Y., Choo, Y.M., Etoh, T., Hayashi, M., Komiyama, K., and Kam, T.S. (2011). Grandilodines A–C, biologically active indole alkaloids from *Kopsia grandifolia*. *J. Nat. Prod.* 74, 1309–1312.
32. Gao, X., Wu, B., Huang, W.-X., Chen, M.-W., and Zhou, Y.-G. (2015). Enantioselective palladium-catalyzed C–H functionalization of indoles using an axially chiral 2,2'-bipyridine ligand. *Angew. Chem. Int. Ed.* 127, 12124–12128.
33. Lian, Y., and Davies, H.M.L. (2010). Rhodium-catalyzed [3 + 2] annulation of indoles. *J. Am. Chem. Soc.* 132, 440–441. Delgado-Rebollo, M., Prieto, A., and Pérez, P.J. (2014). Catalytic functionalization of indoles by copper-mediated carbene transfer. *ChemCatChem* 6, 2047–2052. Gibe, R., and Kerr, M.A. (2002). Convenient preparation of indolyl malonates via carbenoid insertion. *J. Org. Chem.* 67, 6247–6249.
34. Vargas, D.A., Tinoco, A., Tyagi, V., and Fasan, R. (2018). Myoglobin-catalyzed C–H functionalization of unprotected indoles. *Angew. Chem. Int. Ed.* 57, 9911–9915.
35. Ye, F., Qu, S., Zhou, L., Peng, C., Wang, C., Cheng, J., Hossain, M.L., Liu, Y., Zhang, Y., Wang, Z.X., et al. (2015). Palladium-catalyzed C–H functionalization of acyldiazomethane and tandem cross-coupling reactions. *J. Am. Chem. Soc.* 137, 4435–4444.
36. Young, I.S., Thornton, P.D., and Thompson, A. (2010). Synthesis of natural products containing the pyrrolic ring. *Nat. Prod. Rep.* 27, 1801–1839.

37. Chawner, S.J., Cases-Thomas, M.J., and Bull, J.A. (2017). Divergent synthesis of cyclopropane-containing lead-like compounds, fragments and building blocks through a cobalt catalyzed cyclopropanation of phenyl vinyl sulfide. *Eur. J. Org. Chem.* **2017**, 5015–5024. Talele, T.T. (2016). The “cyclopropyl fragment” is a versatile player that frequently appears in preclinical/clinical drug molecules. *J. Med. Chem.* **59**, 8712–8756. Fuerst, D.E., Stoltz, B.M., and Wood, J.L. (2000). Synthesis of C(3) benzofuran-derived bisaryl quaternary centers: approaches to diazomide. *A. Org. Lett.* **2**, 3521–3523. Taylor, R.D., MacCoss, M., and Lawson, A.D.G. (2014). Rings in drugs. *J. Med. Chem.* **57**, 5845–5859. Also see: Salaün, J. (2000). Cyclopropane derivatives and their diverse biological activities. In *Topics in Current Chemistry*, A. de Meijere, ed. (Springer), pp. 1–67.
38. Davies, H.M.L., and Antoulinakis, E.G. (2001). Intermolecular metal-catalyzed carbenoid cyclopropanations. *Org. React.* **57**, 1–326.
39. Lebel, H., Marcoux, J.F., Molinaro, C., and Charette, A.B. (2003). Stereoselective cyclopropanation reactions. *Chem. Rev.* **103**, 977–1050.
40. For review, see: Lipshutz, B.H. (1986). Five-membered heteroaromatic rings as intermediates in organic synthesis *Chem. Rev.* **86**, 795–819. For selected example, see: Lee, H.-K., Chan, K.-F., Hui, C.-W., Yim, H.-K., Wu, X.-W., and Wong, H.N.C. (2005). Use of furans in synthesis of bioactive compounds. *Pure Appl. Chem.* **77**, 139–143.
41. For review, see: van Putten, R.-J., van der Waal, J.C., de Jong, E., Rasrendra, C.B., Heeres, H.J., and de Vries, J.G. (2013). Hydroxymethylfurfural, a versatile platform chemical made from renewable resources *Chem. Rev.* **113**, 1499–1597. For example, see: Mirzaei, H.M., and Karimi, B. (2016). Sulphanilic acid as a recyclable bifunctional organo-catalyst in the selective conversion of lignocellulosic biomass to 5-HMF. *Green Chem.* **18**, 2282–2286.
42. Julis, J., and Leitner, W. (2012). Synthesis of 1-octanol and 1,1-dioctyl ether from biomass-derived platform chemicals. *Angew. Chem. Int. Ed.* **51**, 8615–8619. Xia, Q.-N., Cuan, Q., Liu, X.-H., Gong, X.-Q., Lu, G.-Z., and Wang, Y.-Q. (2014). Pd/NbOPO<sub>4</sub> multifunctional catalyst for the direct production of liquid alkanes from aldol adducts of furans. *Angew. Chem. Int. Ed.* **53**, 9755–9760.
43. Hazra, C.K., Gandhamsetty, N., Park, S., and Chang, S. (2016). Borane catalysed ring-opening and closing cascades of furans leading to silicon functionalized synthetic intermediates. *Nat. Commun.* **7**, 13431–13439.